Preparation of cells for assessing ultrastructural localization of nanoparticles with transmission electron microscopy

Amanda M Schrand[1], John J Schlager[1], Liming Dai[2] & Saber M Hussain[1]

[1]AFRL/711 HPW/RHPB, Wright-Patterson Air Force Base, Dayton, Ohio, USA. [2]Department of Chemical Engineering, Case Western Reserve University, Cleveland, Ohio, USA. Correspondence should be addressed to S.M.H. (saber.hussain@wpafb.af.mil).

We describe the use of transmission electron microscopy (TEM) for cellular ultrastructural examination of nanoparticle (NP)-exposed biomaterials. Preparation and imaging of electron-transparent thin cell sections with TEM provides excellent spatial resolution (~1 nm), which is required to track these elusive materials. This protocol provides a step-by-step method for the mass-basis dosing of cultured cells with NPs, and the process of fixing, dehydrating, staining, resin embedding, ultramicrotome sectioning and subsequently visualizing NP uptake and translocation to specific intracellular locations with TEM. In order to avoid potential artifacts, some technical challenges are addressed. Based on our results, this procedure can be used to elucidate the intracellular fate of NPs, facilitating the development of biosensors and therapeutics, and provide a critical component for understanding NP toxicity. This protocol takes ~1 week.

INTRODUCTION

The recent development of engineered nanoparticles (NPs) has attracted the attention of many individuals from diverse scientific disciplines, who are rapidly pursuing a plethora of exciting and new applications. Concurrently, the implications for potential long-term health and environmental applications are being addressed by various working groups, although at a considerably slower pace[1–4]. In our studies, we focus on the NP toxicity-associated bioeffects that produce acute dose-dependent decreases in viability and alterations in cell function (e.g., membrane leakage, mitochondrial damage, reactive oxygen species (ROS) generation, cytokine production, up- or down-regulation of genes and so on)[5–17]. Certainly, long term or chronic effects will require much further investigation. For an overview of recent bioeffect achievements, challenges and current understanding of NP behavior at the bio-interface, see reviews by our group[18,19] and others[20,21].

In addition to measuring biochemical cell alterations after exposure to NPs, a variety of microscopic methods, ranging from simple light microscopy to more complex electron microscopy, can be used to determine the uptake and intracellular localization of NPs inside cells. For example, we have used an ultrahigh resolution imaging system, which attaches to a standard research-grade inverted microscope for the examination of NP interactions and possible internalization into live cells[7,8,13–15,18]. Frequently, surface-active NPs in agglomerated structures are observed using this method. However, the exact localization of individual NPs inside of the cells was not determined owing to resolution limitations (~150 nm) and the inability to carry out serial sectioning to distinguish membrane-bound versus internalized NPs. Other limitations of live cell imaging with light microscopy include organelle autofluorescence, subtle changes in brightness with NPs found inside or outside of cells and short observation times, which can alter the image interpretation. Fluorescent microscopy suffers many of the same limitations as light microscopy and is limited to NPs that will emit light upon excitation. However, fluorescent microscopy is still a very valuable technique to observe illuminated internalized NPs

while sacrificing the nano-sized vision area. In this case, the relationship between certain organelles, which are usually sized from submicrons to microns, and NPs internalized into those organelles (e.g., endosomes and lysosomes) can be explored[22–24]. In addition, the serial sectioning capabilities of confocal microscopy can be used to identify more qualitatively the uptake of NP agglomerates into certain organelles in living cells. However, there is still insufficient resolution (> 100 nm) to examine individual NPs.

To gain the resolution required to view individual NPs (< 100 nm), electron microscopy is typically carried out. However, fragile biological samples such as cultured cells used in mechanistic studies require dehydration, heavy-metal staining and electron transparency for the sample to withstand the vacuum conditions and generate appropriate signal contrast to form an image. Further limitations of TEM include time consuming and toxic sample preparation, difficulties in distinguishing low-contrast nano-sized materials from cellular background features (e.g., cytoplasmic granules), production of two-dimensional black and white images and difficulty in drawing statistical conclusions. At present, stereological principles are being utilized to quantify the spatial distribution of immunogold and other NPs based on their localization throughout the cells and tissues for statistical evaluation[25]. These studies rely on χ^2 analysis between treatment groups or within a single group to determine differences in uptake amount or localization to specific intracellular compartments. The purpose of these studies is being able to carry out these relative quantification techniques in the TEM in an unbiased manner.

The use of lower voltage imaging with scanning TEM (STEM) in a standard scanning electron microscope (SEM) may generate greater contrast without the use of heavy-metal stains, but requires an electron-transparent sample; hence a protocol involving embedding and thin sectioning is presented. Hydrated samples can be viewed under high vacuum conditions in the SEM if specialized capsules (e.g., from Quantomix, Rehovot, Israel) are used. However, we found that heavy-metal staining was still required to generate

1. REPORT DATE **MAR 2010**	2. REPORT TYPE	3. DATES COVERED **00-00-2010 to 00-00-2010**

4. TITLE AND SUBTITLE	5a. CONTRACT NUMBER
Preparation of cells for assessing ultrastructural localization of nanoparticles with transmission electron microscopy	5b. GRANT NUMBER
	5c. PROGRAM ELEMENT NUMBER
6. AUTHOR(S)	5d. PROJECT NUMBER
	5e. TASK NUMBER
	5f. WORK UNIT NUMBER

7. PERFORMING ORGANIZATION NAME(S) AND ADDRESS(ES) **Case Western Reserve University,Department of Chemical Engineering,10900 Euclid Avenue,Cleveland,OH,44106**	8. PERFORMING ORGANIZATION REPORT NUMBER

9. SPONSORING/MONITORING AGENCY NAME(S) AND ADDRESS(ES)	10. SPONSOR/MONITOR'S ACRONYM(S)
	11. SPONSOR/MONITOR'S REPORT NUMBER(S)

12. DISTRIBUTION/AVAILABILITY STATEMENT **Approved for public release; distribution unlimited**

13. SUPPLEMENTARY NOTES

14. ABSTRACT

15. SUBJECT TERMS

16. SECURITY CLASSIFICATION OF:			17. LIMITATION OF ABSTRACT	18. NUMBER OF PAGES	19a. NAME OF RESPONSIBLE PERSON
a. REPORT **unclassified**	b. ABSTRACT **unclassified**	c. THIS PAGE **unclassified**	**Same as Report (SAR)**	**14**	

Figure 1 | Cellular structures, possible mechanisms of nanoparticle (NP) uptake and some potential NP physicochemical uptake factors. Receptor (R), vacuole (V), mitochondria (M), cytoplasmic granules (CG), cytoskeleton (C), rough endoplasmic reticulum (RER), smooth endoplasmic reticulum (SER), nucleus (N), golgi (G), endosome (E) and lysosome (L). Steps in endocytic uptake (1–4) or nonendocytic mechanism.
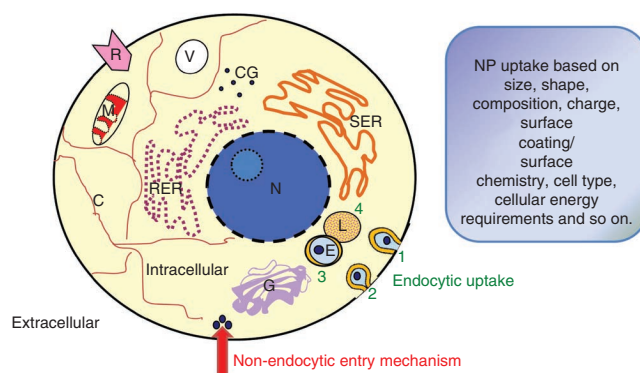
sufficient contrast and that only high atomic number NPs were readily detectable. More recently, de Jonge et al.[25] have unveiled a new STEM-based technique for imaging whole cells in liquid by a microfluidic device with electron-transparent windows[26]. Other groups have used field emission SEM (FESEM) to directly observe nuclear morphologies, including nuclear envelope structures, with immunolabeling or freeze fracture techniques[27–29]. Although alternative electron microscopy and spectroscopic techniques are continuously being developed to combat the artifacts generated during the extensive sample preparation (e.g., fixation, dehydration and heavy-metal staining) required for high vacuum, high-voltage electron beam energy imaging of thin sections in TEM, there are no true comparative methods. Therefore, TEM is routinely used by many groups to determine the uptake and localization of NPs inside cells, as well as provide clues to the uptake mechanism whether it is endocytic[30–37] or not[38] (**Fig. 1**).

In TEM, an electron beam is transmitted through samples typically < 100 nm thick to generate a bright-field (BF) image containing information about the internal structure of the sample. In addition to TEM BF imaging, TEM cryo-microscopy, tomography and other TEM imaging modes (e.g., high-angle annular dark-field imaging, energy-filtered TEM (EF-TEM), electron energy loss spectroscopy and aberration corrected STEM)[39–41] can image unstained or stained cells. The sample preparation techniques can include freeze substitution and freeze drying[42,43] with the cells grown directly on Au TEM grids coated with various biomolecules (e.g., L-lysine, fibronectin and laminin)[44,45]. Subsequent thinning of frozen samples can be accomplished after embedding in resin[46] or with a focused-ion beam instrument[47]. Therefore, nanomaterials and cell components, such as organelles, can be clearly imaged by TEM once they have been correctly prepared. Here we present our current protocol for streamlining the preparation of cells for TEM analysis after dosing with NPs using traditional dehydration, embedding and thin sectioning procedures. The information gained from thin sections of cells incubated with NPs is critical for understanding the interaction and underlying mechanisms involved in their uptake, associated applications and potential toxicity.

Experimental design

Cell types. A multitude of cell lines are currently available that can represent target organs of NP exposure (e.g., lung and skin) or have clinical relevance (e.g., cancer cells versus normal cells). During our studies with multiple cell types, we began to notice several important differences in their innate response to NPs regarding internalization mechanism and degree of inflammatory cascade. We demonstrated that immune cells (e.g., alveolar macrophages) display differential toxicity to various carbon nanomaterials compared with neuroblastoma cells; possibly due to greater NP accumulation[10]. Other recent studies have revealed similar cell-specific trends in toxicity and uptake[21,48–54] as well as noting the importance of NP uptake during certain stages of the cell cycle in differentiated

versus non-differentiated cells and cells with shorter versus longer doubling times[54]. These factors and more should be taken into consideration when choosing a cell line for NP research. However, no one particular cell type is currently favored for NP-uptake studies. Further, the cell line chosen for toxicity studies should be based upon the potential target organ or application.

General characterization techniques for NPs. For the NPs in these studies, characterization was accomplished with TEM for size and morphology, inductively coupled plasma–optical emission spectroscopy for purity, dynamic light scattering (DLS) for hydrodynamic radius in solution and zeta potential to estimate charge in solution. The lack of sufficient pre-exposure characterization details in NP-dosing studies is being addressed in many different ways. Analysis using 'dry' characterization is being carried out to determine initial primary size, mono- or polydispersity of the size distribution, length, diameter, surface area, elemental composition/trace impurities, crystallinity, etc. However, once the NPs are introduced into cell-culture media, their surface properties change because of interactions with water and aqueous solution salts, small organic molecules, proteins and other cell constituents. These solution interactions can affect NP cellular dynamics by immediate and dynamic surface-modification effects such as material size, surface chemistry and delivered dose, which are likely different for each NP composition. A clear understanding of NP surface dynamics remains poorly understood and still is a significant hurdle to overcome in this field. In addition to the characterization techniques mentioned above, further microscopic solution characterization such as cryo-electron microscopy or computer modeling on the forces contributing to NP interactions with media components, cell membrane and intercellular environments (e.g., van der Waals forces, electrostatic double-layer interactions, short-range forces arising from charge, steric hindrance, NP dissolution, ion leaching, phase transformation and solvent interactions and so on), are being explored[21]. However, it is not the focus of this protocol to impose a particular set of NP parameters on the experimenter, but rather to provide some general handling guidelines for NP-uptake studies.

NP types. The different types of NPs that we have studied include, but are not limited to, the following: manganese (Mn), silver (Ag), single-walled carbon nanotubes (SWNTs), multi-walled carbon nanotubes (MWNTs), nanodiamonds (ND), carbon black (CB), silica (SiO_2), aluminum (Al), aluminum oxide (Al_2O_3), titanium dioxide (TiO_2), copper (Cu) and gold (Au). For demonstration purposes, we chose a few different carbon-based NPs (NDs (1),

CB (2) and SWNT and MWNT (3)) to demonstrate their uptake into neuroblastoma (N2A) cells.

1. *NDs*: The NDs used in our laboratory were generously supplied by NanoCarbon Research Institute in Nagano, Japan and were synthesized according to previously reported detonation techniques[55,56]. The NDs had primary sizes of 5.1 ± 1.7 nm with 0.13 wt% Fe and 0.23 wt% Zr impurity content from the detonation container and bead milling. They formed strong aggregates in water of ~158 nm that dramatically increased in size to 2,180 nm in cell-culture media. The charge measured with zeta potential was ~43 mV.

2. *CB*: CB NPs used in our research were received from Shell/ Cabot (Boston, MA, USA) and were synthesized using an oil furnace process. As furnace-type CB NPs are made from petroleum feedstocks, CB can contain varying amounts of other elements (e.g., sulfur), up to 1 wt%. The CB NPs had primary sizes of 28.8 ± 8.4 nm and 0.43 wt% sulfur-impurity content. Because of van der Waals forces, they readily form very strong aggregates in aqueous solutions. For example, CB NPs have much larger sizes in water (an average of 396 nm) than their primary size of ~30 nm. Further, CB analyzed in DMEM/F-12-dosing cell-culture media (no serum) produced aggregates of ~2,190 nm.

3. *MWNTs and SWNTs*: MWNTs were purchased from Tsinghua University (Beijing, China) and SWNTs were received from Rice University (Houston, TX, USA). SWNTs and MWNTs were synthesized by chemical vapor deposition. The maximum lengths of both the SWNT and MWNT were not as readily calculated owing to bundling and tangling. The SWNTs existed in bundles that were greater than 3 µm in length with bundle diameters of ~25 nm, whereas individual SWNT diameters were 1–3 nm. The MWNTs were estimated to be from 0.5 to 40 µm in length with diameters from 9–40 nm. The MWNTs had a residual Fe catalyst content of 0.49 wt%, whereas the SWNT had a residual Fe catalyst content of 0.26 wt%. The DLS size approximation is based on a spherical particle assumption for calculation, so the results for SWNT and MWNT solutions would not be meaningful due to NT disparity of diameter and length creating. The results show high polydispersity reading. For example, in water the SWNTs had a mean size of ~900 nm and MWNTs ~821 nm. The zeta potential of the SWNTs was 50.2 mV compared with − 13.6 for MWNTs.

Additional chemicals or treatments for NP dispersion. Although some newly engineered NPs show enhanced stability in biological media[57,58], the issue of NP agglomeration in cell-culture media before dosing cells is a well-known phenomenon and there is not a common solution capable of suspending all types of NPs. To examine dispersion in aqueous stock solution medium before dosing cells, we have used high illumination light microscopy[7,8] and DLS[15]. Other techniques to examine or modify dispersion include the addition of surfactants[8,59] and centrifugation[30,60–63]. The latter may serve a second role to filter out possible bacterial contaminants[30]. However, we do not use surfactants or any form of centrifugation before dosing to avoid problematic interference with the inherent surface chemistry of the NPs, which would mask NP surface bioeffects and provide potential cytotoxic effects of surfactants on the cells[8,59]. Centrifugation can force overall
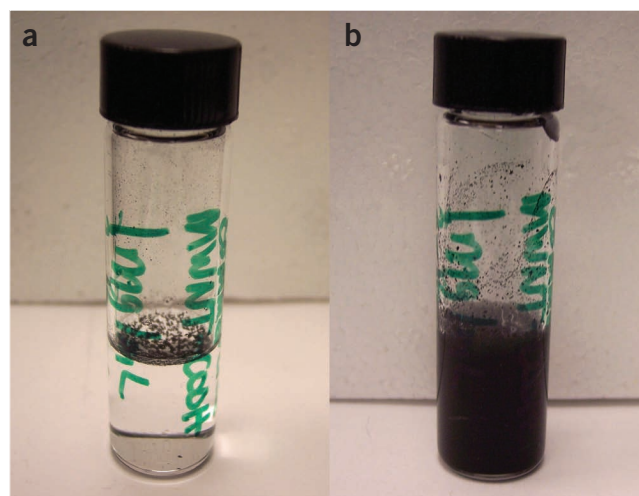
Figure 2 | Issue of nanoparticle (NP) agglomeration and dispersion. Multi-walled carbon nanotubes (MWNTs) added to water. (**a**) Before sonication where the hydrophobic nature causes the MWNTs to aggregate at the surface of water. (**b**) After sonication where the MWNTs are temporarily suspended in the water before dilution in cell-culture media.

physical size change effecting NP surface and concentration dosing by irreversible agglomeration. To combat agglomeration, we typically employ a brief sonication to disperse materials such as carbon nanotubes (**Fig. 2**). Although conventional sonication in water baths or with probe-tip sonicators has extensively been used to disperse NPs, new techniques such as bead-assisted sonic disintegration have been demonstrated to break up persistent agglomerates of NDs concurrent with surface functionalization[57]. However, chemical-surface modification achieved through extensive sonication or very high-energy sonic pulses may markedly change the NP surface characteristics and should be avoided. Teeguarden *et al.*[64] provide a further discussion of the influence of NP and cell-culture media characteristics on dosimetry.

Cell and NP controls. Control cells that are not dosed with NPs but with dosing media only are required for comparison of processed samples for TEM. In toxicological studies, CB has frequently been used as a negative control and we have employed micron-sized cadmium oxide as a positive toxic substance control. However, these materials must also be considered thoughtfully for application and comparison. The heterogeneous nature of different CB samples has been addressed by the Monteiro group and others for significant variability depending upon the acquired source. The US National Bureau of Standards, now called the National Institutes of Standards and Technology, is currently developing suitable standard reference materials (SRM). The most likely SRM candidates include nonactive materials such as Au (10, 30 and 60 nm) or polystyrene (60 and 100 nm) spheres, which have very narrow size distributions (http://www.nist.gov). Other solutions to test as controls can include additives such as surfactants or surface coating components separate from the NPs. Other considerations for toxicity controls can include cells not stained, examination of the NPs without cells and examination by independent laboratories to confirm the results[53]. However, in NP-uptake studies, the best 'control' is to prepare and image cells that have not undergone any experimental treatment but that are handled and prepared in exactly the same procedure as the NP-dosed cells.

Length of treatment time. The length of treatment time can depend upon the toxicity of the NP, cell type and purpose of the experiment. For example, low-toxicity NPs may be able to accumulate over days without significant changes in cell adherence or morphology, leading to a sample suitable for further processing for TEM. For example, quantum dots were used to noninvasively label *Dictyostelium* or HeLa cells for over 12 d without affecting cell growth or development[65]. In contrast, highly toxic NPs may lead to cell rounding and detachment from substrates with highly vacuolated cytoplasms and may not be ideal for further processing for TEM. In cell types that have a greater propensity for NP uptake (i.e., macrophages, monocytes and neutrophils), shorter time points should be considered (see previous discussion of cell-specific differences). In contrast, for experiments designed to elaborate upon the mechanism of NP entry, accumulation and exit, a time course approach from 1 to 24 h or longer can be utilized. For cytotoxicity analysis, Lanone *et al.*[53] suggested that the 24 h time point (versus 3 h) provided more sensitive data. In agreement with this study, the Monteiro group recommends toxicity assays continue for at least 24 h to complete one cell cycle, with 24 h being a common cultured-cell doubling time and after 48 h, one finds further decreases in cell viability[66]. Issues that the researcher can expect to address in studies > 24 h include cell proliferation, microbial growth and possible removal and reapplication of dosing solutions. Therefore, in this protocol we suggest a dosing period of 24 h or shorter.

Concentrations of NPs. The calculation of NP dose has been carefully considered, and to date most studies employ a mass-basis approach compared with surface area calculations, which may or may not accurately represent the interface of the NPs with individual cells. Support for the mass-basis approach can be found in a study by Limbach *et al.*[60], where cerium oxide NPs introduced into human lung fibroblasts reveal a strong dependence of the amount of incorporated ceria on particle size, whereas NP number density or total-particle surface area showed weaker correlations. Other studies have found no correlation between toxicity and either specific surface area or equivalent spherical diameter[53,67,68]. However, some studies in animals show a good correlation between the NP surface area and inflammatory response[68–71]. NPs such as Au NPs[72,73] or quantum dots (QDs)[74] can be expressed in 'molarity'. In the case of QDs, molarity refers to an entire quantum dot with concentrations of Cd in 20 μM stock solutions translating to ~38,000 μM (refs. 23,74). The concentration range for dosing in uptake studies can be based upon toxicity data, which for most of our studies is between 0–100 μg ml^{-1} (refs. 5–19). A survey of the existing literature demonstrates similar concentration ranges from 0.001 μg ml^{-1} up to 400 μg ml^{-1} (refs. 23,35,75,76) or alternatively 5–100 nM for Au or ceria NPs[73,77].

Electron microscopy preparation and imaging considerations. Each step of the sample preparation process (e.g., fixation, dehydration, resin embedding and so on) can have a great impact on the quality of the resulting sample. In general, fixatives are required to stabilize the structure of the cells during the transition from living, dynamic entities to static, rigid, cross-linked structures so that they can withstand the subsequent dehydration and embedding processes. A solution of buffered formaldehyde and glutaraldehyde (sometimes called Trump's or Karnovsky's fixative) along with osmium tetroxide for post-fixation are commonly employed as fixatives. The benefits of using a mixture of paraformaldehyde
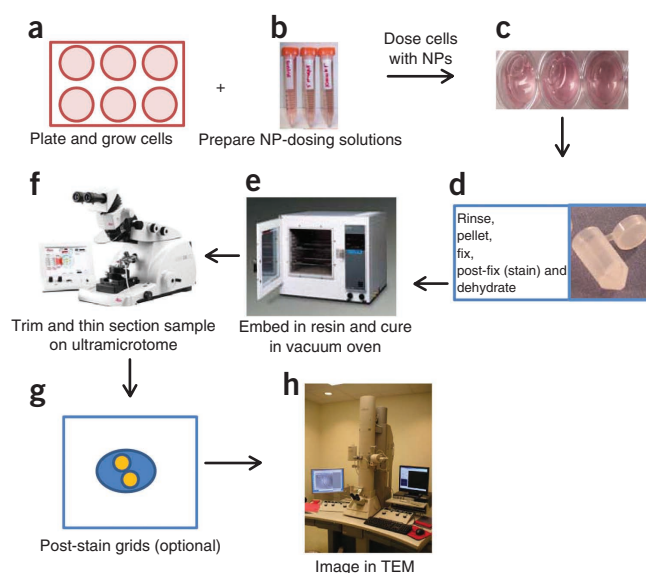
and glutaraldehyde include the ability of paraformaldehyde to quickly stabilize the protein structure through crosslinking and glutaraldehyde to more slowly and permanently fix the cells (more crosslinking) for better preservation of tissue for both light (histological staining) and electron microscopy[78,79]. Glutaraldehyde fixation alone may not be sufficient because lipids and other cell components may not be fixed. Although the aldehyde component is the major preservative of proteins, the later post-fixation with osmium tetroxide helps to preserve lipids well and proteins to some extent. Fixation artifacts typically include extraction of material, distortion of organelles, displacement of chemical components and anomalous deposits (see Troubleshooting section for potential artifacts and remedies). It is beneficial, but not necessary, to use a rotator during the fixation and embedding procedure to ensure thorough mixing and penetration.

For cell isolation, most cells are grown adherent and must be enzymatically or mechanically detached. However, there is not a well-defined speed to centrifuge cells into a pellet for TEM processing. Although we utilize a centrifugation speed of 1,000*g* in our studies, higher speeds have been reported in the literature with good results. For example, Nativo *et al.*[73] used a speed of 5,000*g* and the Monteiro–Riviere group typically uses a very rapid 10 sec spin on a microcentrifuge at 12,500 r.p.m. at 21°C (personal correspondence). Apart from damage to the cells at high centrifugation speeds, there is some concern that centrifugal forces could contribute to unwanted interactions between the NPs and cells. In our studies, the cells are grown as a monolayer and thoroughly washed, leaving very few NPs behind to contribute to sedimentation or artificial penetration. Further isolation of the cells in an agar pellet may reduce these unintended interactions. For example, embedding the cells in 2–3% molten agar before post-fixation with osmium tetroxide may be helpful for cells that are not adherent or to aid in transferring the pellet during various steps of the preparation process[22–24,59,66,73,80–82]. Once the cells are in the form of a pellet, the replacement of the aqueous portion of the cell with ethanol (dehydration series) helps the resin to efficiently penetrate into the cell. However, both dehydration and resin embedment can contribute to protein denaturation and lipid solubilization, so exposure to solvents and embedding media should be as brief as possible. The advantages of using ethanol for dehydration (compared with acetone) include no hardening of the sample and less extraction of cellular components. Further, traces of acetone can act as a radical scavenger and interfere with LR White resin polymerization during curing.

The main purpose of the resin is to provide a solid support for the cells to facilitate the preparation of ultra-thin sections. Resins can be products, such as LR White (acrylic), Epon or Spurr's (epoxy-based), which should be prepared and cured according to the manufacturer's directions. The benefits of epoxy resin include minimal extraction of cellular components, good sample infiltration, uniform polymerization without significant shrinkage artifacts, favorable staining characteristics and stable sections that can withstand the intense heat and vacuum of the TEM. However, we predominantly use LR White resin, which is a one-part formulation with extremely low viscosity, low extraction rate and lower toxicity in both monomeric and polymerized states compared with many epoxy formulations. Therefore, the critical properties of the resin include its viscosity for properly infiltrating the sample, toxicity of the components as well as stability under the

PROTOCOL

electron beam. However, there is no preferred embedding media for cell–NP-uptake studies at this time and a literature survey finds that LR White[39–41], Epon[30,38,54,72,75,83], Spurr's[24,35] or Polybed812 epoxy resin[76,77] are popular formulations. For most resin formulations, increasing both the viscosity and rate of infiltration can be easily accomplished by placing the specimen in a dedicated vacuum oven, with the added advantages that trapped air bubble release and decreased infiltration time can occur simultaneously.

Once thin samples have been carefully prepared on the ultramicrotome and collected onto TEM grids, some imaging conditions in the TEM may need to be optimized for the particular type of NP or staining procedure used. In our studies, NPs are readily visible in the cytoplasm or intracellular vacuoles (endosomes) with sufficient contrast at 80–100 kV in BF-imaging mode. However, in BF-TEM, NPs with higher atomic numbers will appear darker in contrast compared to lower atomic number or less electron-dense polymer NPs or smaller carbon NP structures such as fullerenes. Changing the imaging mode to STEM can improve the contrast of cells and can be combined with EF-TEM. For example, further contrast enhancement of carbon NPs within the carbonaceous cellular matrix was obtained by using low-loss electrons that allowed a clear differentiation between C60 and unstained cellular compartments and also between ordered and disordered forms of aggregated C60 in human monocyte macrophages[39]. In contrast to this work, we consistently use an osmium-based stain for the cellular matrix to generate contrast, as does the Monteiro–Riviere group. This processing allows visualization of various carbon-based NPs and quantum dots. Contrast can also be generated using image processing techniques, but the thickness of the ultramicrotomed sections should remain < 100 nm to assure best results. An overview of the steps in the TEM sample preparation process is shown schematically in **Figure 3**.

Figure 3 | Overview of sample preparation process (**a**–**h**). Plate and grow cells (**a**), prepare nanoparticle (NP)-dosing solutions (**b**), dose cells with NPs (**c**), cell processing (**d**), resin embedding and curing (**e**), trimming of sample, thin sectioning (**f**), optional staining (**g**) and imaging with TEM (**h**).

MATERIALS

REAGENTS
• Cells (from American Type Culture Collection (ATCC)) (see REAGENT SETUP)
• Cell scrapers (Fisher, cat. no. 08-773-2)
• DMEM cell-culture media (Fisher, cat. no. BW12604F) (see REAGENT SETUP)
• 1% Penicillin–streptomycin antibiotic (Sigma Chemical, cat. no. P4333) (see REAGENT SETUP)
• Fetal bovine serum (FBS) normal (ATCC, cat. no. 30-2020) (see REAGENT SETUP)
• Phosphate-buffered saline (PBS) (Invitrogen, cat. no. 70013-032)
• NP suspensions (see REAGENT SETUP)
• 4% Paraformaldehyde fixative (EM Sciences, cat. no. RT 157-4) (see REAGENT SETUP)
• 8% Glutaraldehyde fixative (EM Sciences, cat. no. 16020) (see REAGENT SETUP)
• Osmium tetroxide, 4% aqueous solution (EM Sciences, cat. no. 19150) (see REAGENT SETUP) ▲ CRITICAL Fixatives should be EM quality. Only buy small amounts at a time and use as soon as possible.
• Histology-grade ethanol (Fisher, cat. no. A495F) ▲ CRITICAL Small levels of impurities in ethanol can contribute to premature sample curing.
• Lead citrate (EM Sciences, cat. no. CAS #512-26-5) (see REAGENT SETUP)
• Phosphotungstic acid (EM Sciences, cat. no. 19502-1) (see REAGENT SETUP)
• Uranyl acetate (see REAGENT SETUP)
• LR White resin-medium grade (EM Sciences, cat. no. 14380)
Note: Acrylates can be more hydrophilic and have lower viscosities for easier penetration.

EQUIPMENT
• Culture flasks or plates, such as 6-well cell culture plates (Fisher, cat. no. 08-772-1B)
• BEEM capsules (EM Sciences, cat. no. 70000-B) (see EQUIPMENT SETUP)
• Perfect loop (EM Sciences, cat. no. 70944)
• Formvar/carbon Cu grids 300 mesh (EM Sciences, cat. no. FCF300-Cu)
▲ CRITICAL It is important to have a supporting film on grids for thin cell sections that are delicate, beam-sensitive materials. A combination of both carbon and formvar (polymer) coating of 300-mesh size is desirable for maximum thermal contact of the specimen with the grid to contribute to electron beam stability.
• Fine-tipped tweezer (EM Sciences, cat. no. 78518-3, ultra-fine)
• Syringe filters 0.22-μm (Fisher, cat. no. 09-719A)
• Biological hood (Baker)
• Aspirator and pump (Fisher, cat. no. 01-055-13)
• Micropipetters (Eppendorf)
• Cell incubator (GSS)
• Analytical mass balance (Denver Instrument)
• Probe-tip ultrasonicator (Cole Parmer)
• Water filtration system (Millipore)
• Vortex mixer (Fisher, cat. no. 02-215-365)
• Microcentrifuge (Eppendorf)
• Vacuum oven (Fisher Scientific)
• Light microscope (B&B Microscopes, Olympus, cat. no. CKX31)
• Glass knife (see EQUIPMENT SETUP)
• Diamond knife (Diatome) (see EQUIPMENT SETUP)
• Ultramicrotome (Leica Ultracut) (see EQUIPMENT SETUP)
• TEM (see EQUIPMENT SETUP)

REAGENT SETUP
Cells Murine neuroblastoma (N2A) cells were a kind gift from Dr. David Cool of Wright State University, Dayton, OH, USA. N2A cells were grown in DMEM–F12 media with 10% FBS as previously described[9–10,13]. Cell-culture media, penicillin–streptomycin and other chemicals were purchased from Sigma Chemical (St. Louis, MO, USA). Media contained 1% penicillin–streptomycin as an antibiotic. The cells were maintained in a 5% CO_2 incubator at 37 °C and 100% humidity. Cells are typically grown to at least 70% confluency before dosing.

© 2010 Nature Publishing Group http://www.nature.com/natureprotocols

npg

748 | VOL.5 NO.4 | 2010 | **NATURE PROTOCOLS**

Cell-culture media Combine DMEM media, antibiotics and serum for growth media or prepare media without serum (dosing media) for NP-working solutions.

NP suspensions MWNT and SWNT, nano-sized CB and NDs are weighed in a dry powder form on an analytical mass balance, then suspended in deionized water at a concentration of 1 mg ml^{-1} and retained as stock solutions. Stock NP solutions (1 mg ml^{-1}) are diluted into cell-culture media to working solutions with concentrations from 0 to 100 µg ml^{-1}. Sonicate working solutions for 30 s at 35–40 W if necessary for better dispersion (**Fig. 2**). For more detail, please refer to the Experimental design section.
▲ CRITICAL It is not recommended to use toxic solvents for dispersion, such as tetrahydrofuran (THF), acetone, ethanol and so on, which may affect cell morphology, including membrane permeability and viability, and may lead to incorrect interpretations of NP localization. ❗ CAUTION Wear protective equipment such as disposable respirators (also called dust masks with a recommended N95 filter rating) and goggles to avoid inhalation or mucous membrane contact with dry powder forms of NPs and avoid dermal contact with either powder or solution forms.

Fixative Make fresh fixative by combining glutaraldehyde and formaldehyde in PBS at final concentrations of 2.5% each. ❗ CAUTION Use caution when working with fixatives. Work in a well-ventilated area and use correct disposal methods. Prepare fresh and use immediately with minimal storage time because of fast deterioration.

Osmium tetroxide Dilute the osmium tetroxide in PBS[84] to 1% as a post-fixative (equal parts PBS and 2% osmium tetroxide).

Optional post-staining solutions As multiple thin sections are collected, a post-staining step for enhanced contrast can be carried out. Typically, a combination of uranyl acetate–lead citrate[85], phosphotungstic acid or other stains can be used at this stage (see protocol by Graham and Orenstein[86] for further details). Application of 0.5% aqueous uranyl acetate at 4 °C for 12 h or a higher concentration for a shorter incubation time (e.g., 2% for 1 h) is recommended. ❗ CAUTION Heavy-metal stains (e.g., osmium tetroxide, uranyl acetate, lead citrate and so on) are highly toxic; use with care.

EQUIPMENT SETUP
BEEM capsules BEEM capsules are polyethylene molds with a hinged lid closure and pre-shaped tips that allow more efficient sectioning because of less trimming time. However, they are not reusable and must be cut or popped out before sectioning. Alternative embedding molds include gelatin capsules and multi-use embedding molds (e.g., flat coffin-style molds). Carefully label the BEEM capsule with permanent marker or colored tape that will not be degraded by solvents such as ethanol.
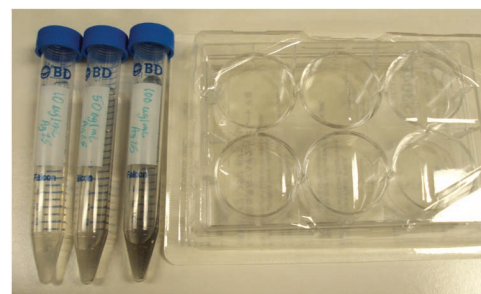
Glass knife Prepare glass knives according to the glass knife machine instructions. Other tools to enhance trimming can include the Leica EM TRIM2 specimen trimmer, which can help prepare better samples faster and more accurately with a tungsten carbide or diamond tool. Combined with a HEPA filter, the EM TRIM2 catches even the smallest particles. Otherwise, debris from the trimming process can be dusted away with pressurized air.

Diamond knife The final sectioning is carried out with a diamond knife on the ultramicrotome set with the manufacturer's provided clearance angle (typically 4–6°). Carefully inspect the knife edge under a stereomicroscope with back illumination for chips or other damage as well as fingerprints or other contamination. Securely fasten the sample into a holder. Adjust the level of water until the reflection from the surface becomes a silver tint before starting to produce sections on water.

Ultramicrotome Set section parameters (speed and thickness) by programming the unit accompanying the ultramicrotome. First set the cutting window (upper starting point and lower ending point) and the automated section thickness to several 100 nm until full sections are being cut at a speed between 1 and 2 mm s^{-1} or simply use manual advancement.
▲ CRITICAL The ultramicrotome should be properly assembled on a solid table (e.g., slate or concrete) in an area where vibrations, drafts and temperature fluctuations are minimal.

TEM Set the instrument at 75–80 kV or other suitable kV such as 100 kV. However, lower kV imaging, with the beam well spread, is preferred to avoid damage to the delicate thin sections.

PROCEDURE
Plate and grow cells ● TIMING 24–48 h
1| Grow cells according to the established techniques, then plate in 6-well plates (area = 9.5 cm^2) to obtain a sufficient cell number to prepare a 1-mm^3 pellet (~10^6 cells or more) (**Fig. 4**).
▲ CRITICAL STEP Knowledge of cell-growth time is required and can be determined by calculating the dividing rate from successful seeding densities (obtained from detaching adherent or vital dye (trypan blue) for viable cells and counting within 2–4 h post-seeding) and the amount of viable cells after growth for 24–72 h, depending on the cell line.
? TROUBLESHOOTING

Prepare NP-dosing solutions ● TIMING 30 min
2| Prepare the final dosing solutions in the appropriate cell-culture media.
▲ CRITICAL STEP The type of media chosen for suspension of a particular NP will coincide with the cell type to be dosed and typically contains no or reduced serum (to discourage extensive cell growth). The final size of NPs in dosing media may vary markedly from the primary NP size and can be examined with techniques such as dynamic light scattering. Furthermore, sonication or surface functionalization may be able to mitigate NP aggregation.
? TROUBLESHOOTING

3| Add any surfactants or other solvents to the NP suspension if necessary.
▲ CRITICAL STEP If additional chemicals are utilized to disperse the NPs, testing of the chemicals for cell viability changes is suggested (e.g., MTT viability assay), as well as using aseptic technique and sterilized solutions.
? TROUBLESHOOTING

Dose cells with NP ● TIMING 1–24 h
4| Transfer cells from the incubator to the biological hood and aspirate the growth media from the cells.

Figure 4 | Image of diluted nanoparticle (NP) solutions and 6-well plate used in cell-dosing studies.

▲ **CRITICAL STEP** For cells in suspension, centrifugation may be necessary to retain the cells during subsequent rinsing steps. For cell lines that easily get dislodged during rinsing, previous coating of the 6-well plate with collagen or other binding agents may be necessary or embed the cells in agar.
? TROUBLESHOOTING

5| Briefly vortex (10 s) the NP-dosing solution to enhance dispersion, then add 1 ml to each well in the 6-well plate with a micropipetter.
? TROUBLESHOOTING

6| Return the dosed cells to the incubator for 24 h or other appropriate exposure time.

Cell processing: rinse, pellet, fix, post-fix (stain) and dehydrate ● TIMING 24 h
7| Thoroughly rinse the NP solution from the cells with fresh dosing media (containing no serum or reduced serum content) at room temperature (21 °C) 2–3 times for at least 5 min each time. This step can be carried out on a stir plate for enhanced rinsing. Low centrifugation 200–2,000g at 21°C in a polypropylene 15–50 ml conical tube to pellet cells with two to three re-suspending washes of the cell pellet can be used for lightly attached or suspended cells. This will separate the suspended NPs from the cell pellet.
? TROUBLESHOOTING

8| Aspirate the media after the last wash or return suspended cells in culture media to culture plate or flask in growth media.

9| For adherent cells, use a standard technique to release the cells (e.g., pipette, trypsinize or scrape), depending upon their adherence, from the wells and pipette into labeled BEEM capsules (with pre-formed trapezoid shape).

10| Centrifuge the cells for 5 min at 1,000g at room temperature to form a pellet at the bottom of the capsule.
! CAUTION Centrifugation of the sample before fixation may cause some distortion to the cellular contents, with greater damage occurring at higher centrifugation speeds. However, it is important to maintain a pellet throughout the fixation, dehydration and rinsing steps to have enough cells for proper resin embedding. Repeated centrifugation is not recommended but can be carried out if the pellet is disrupted.
▲ **CRITICAL STEP** The pellet size should be between 0.5 and 1 mm, which is approximately 1 million cells. If it is larger, separate a portion of the pellet before continuing with the fixation.
? TROUBLESHOOTING

11| Add ~1 ml of fresh 2.5% glutaraldehyde/formaldehyde in PBS at room temperature for 2 h.
▲ **CRITICAL STEP** Other suitable EM quality fixatives can be used, but the same buffer that the fixative is diluted in should be used for rinsing.
▲ **CRITICAL STEP** Do not use old fixatives (typically, fixatives are only good for ~1 week).
? TROUBLESHOOTING

12| Thoroughly rinse with PBS, three times for 10 min each, after fixation is complete.

13| Add ~1 ml of 1% osmium tetroxide in PBS to the cell pellet for 1 h.
▲ **CRITICAL STEP** Osmium tetroxide will penetrate most samples at a rate of 1 mm h^{-1}. However, extended times in this fixative may cause unwanted protein extraction, so the immersion time should be kept to a minimum.
! CAUTION Fixatives are designed to react with biological materials and extreme caution should be taken when handling them. Osmium tetroxide, e.g., can fix the cornea of the eye. Use in a well-vented biological hood and wear protective clothing. Dispose of any unused osmium in the hazardous waste stream; add corn to opened one-time use glass ampoules for retention of material.
? TROUBLESHOOTING

14| Rinse pellet in the same buffer as the fixative diluent (e.g., PBS) five times for 10 min each and then double-distilled water (ddH$_2$O) two times for 10 min each. An optional step at this stage is to stain samples *en bloc* in 0.5% aqueous uranyl acetate for increased contrast (4 °C for 12 h); a higher concentration for shorter time can also be used (e.g., 2% for 1 h). After staining, rinse well in distilled water. However, this optional staining step may be more convenient after the thin sections are made and placed on grids. Continue at Step 41.
? TROUBLESHOOTING

Dehydration series ● TIMING 5–15 min

15| Remove ddH$_2$O and start dehydration through a graded series of ethanol concentrations (50, 70, 90 and 100%) for 5–15 min each. These steps can be carried out on a stir plate to ensure thorough penetration and equilibration.

▲ **CRITICAL STEP** The dehydration steps are critical for replacing the water in the sample with ethanol, which is miscible with the embedding resin. At no point should the samples be allowed to air dry.

! **CAUTION** Ethanol is flammable.

■ **PAUSE POINT** Samples can be left in 70% ethanol overnight if necessary and the dehydration process continued till the next day.

? **TROUBLESHOOTING**

Resin embedding and curing of the cell pellet ● TIMING 24 h

16| Add a 50:50 resin:ethanol mixture for 30–45 min or longer.

▲ **CRITICAL STEP** It is not necessary to dilute LR White with ethanol and if histology-grade ethanol is not used, premature curing may occur from impurities; if this occurs, continue to Step 18 for overnight infiltration. Take care to avoid the formation of bubbles during resin mixing by stirring slowly.

17| Replace the diluted resin mixture with 100% resin (can heat to 40–60 °C if appropriate for curing, but not necessary for LR White).

18| Allow resin to infiltrate into the sample overnight (~15 h).

! **CAUTION** Cold curing of osmium-fixed cells with an accelerator is not recommended.

! **CAUTION** Resins should be treated as potential toxins and mutagens, with care taken to avoid dermal contact or inhalation of the vapors in the liquid phase or the dust from the polymerized blocks. All work should be carried out in a well-ventilated area while wearing gloves. Polymerization should occur in a vacuum oven vented to the building exhaust system. It is recommended that unused resin be polymerized before disposal according to safety guidelines.

▲ **CRITICAL STEP** Typically, epoxy resins are compatible with ethanol, and no transition media is needed, but they are hydrophobic and should be maintained free of water. For resins poorly miscible in ethanol, an intermediate step including a miscible agent (e.g., propylene oxide) can be included. Add a 50:50 mixture of propylene oxide and ethanol for 5 min, then 100% propylene oxide for 10 min, followed by a 50:50 mixture of propylene oxide:resin for 45 min before continuing in 100% resin overnight.

▲ **CRITICAL STEP** Increasing the viscosity (and rate of infiltration) can be easily accomplished by placing the specimen in a dedicated vacuum oven where the added advantages of trapped air bubble release and decreased infiltration time occur simultaneously. If the sample appears to be soft or tacky, continue curing before trimming or sectioning.

? **TROUBLESHOOTING**

Trimming of sample ● TIMING 30 min–1 h

19| Prepare the sample block face after the cells have been embedded and cured. If a BEEM capsule was used, the block face may already be sufficiently prepared (e.g., small in size, flat face and cells reach bottom of capsule). Otherwise, follow the steps below and consider standard references for detailed instructions[87]. An example of the sample and equipment used for the thin sectioning portion of the protocol is shown in **Figure 5**.

▲ **CRITICAL STEP** If the cells do not reach the tip of the BEEM capsule, first attempts to obtain thin sections will not yield embedded cells. It is recommended to shave away some of the resin first with a glass knife, then proceed to ultrathin sections with the diamond knife.

20| Trim away large areas of resin/sample (if necessary) with a razor blade (first cleaned with solvent to remove grease).

! **CAUTION** Take care when trimming blocks by hand with a razor blade. Use an up and away motion to shear off resin.
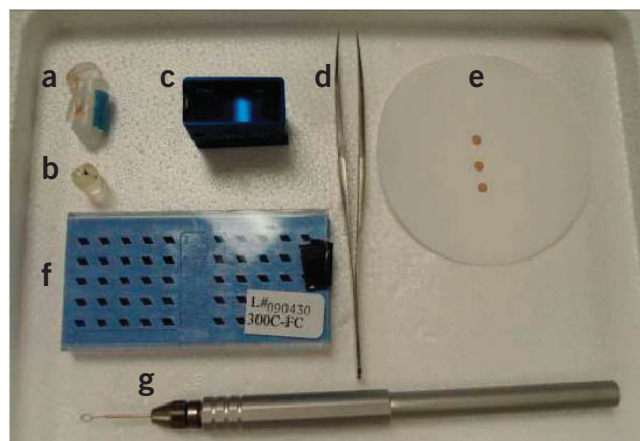
Figure 5 | Sample and equipment used for thin sectioning of resin-embedded cells (**a–g**). BEEM capsule (**a**), cured resin-embedded sample from BEEM capsule (**b**), diamond knife (**c**), fine-tipped tweezers (**d**), formvar-carbon coated TEM grids on Whatman's paper (**e**), TEM grid-storage box (**f**) and perfect loop (**g**).

21| Securely fasten the sample to a trimming block or holder that accompanies the ultramicrotome.

22| Adjust the stereomicroscope lenses to the lowest magnification and set lighting to focus on the sample.

23| Insert the glass knife into the knife holder and position in close proximity to the sample block face.

24| Trim by manually advancing the glass knife attached to the ultramicrotome while viewing the sample through the stereomicroscope lenses.

25| Rotate the sample and knife to produce a final trapezoid shape ~1-mm or less in size.
! CAUTION Make sure that the sample and glass knife are securely fastened and avoid steep trimming angles.
? TROUBLESHOOTING

26| Remove knife from holder and either store in glass knife box or discard in sharps container.

27| Clean ultramicrotome area of resin shavings.

28| Optional: obtain thin sections with a glass knife modified with tape to make a water bath (then continue below).

Thin sectioning on ultramicrotome with a diamond knife ● TIMING 30 min–1 h
29| Insert diamond knife in knife holder and lock in place.

30| Move sample and knife in close proximity while viewing the sample through the stereomicroscope lenses.

31| Fill diamond knife trough with water from a syringe until the surface of the water reflects a silver color (thus indicating water is parallel to the knife edge).
? TROUBLESHOOTING

32| Increase stereomicroscope magnification to align lighting with a view of the block face and knife-edge. The bottom edge of the block face should be parallel with the knife-edge.

33| Set the upper and lower portions of the cutting window for automated sectioning.

34| Set the section speed at 1 mm s^{-1} for automated sectioning.

35| Set the section thickness at 200 nm or greater to allow the block face to become parallel to the knife-edge for a full section.

36| Begin sectioning by either manually advancing the cutting wheel or by pressing start on the automation.
▲ CRITICAL STEP The initial sections will be thicker than required for the final sections. The color of thicker sections may be purple or blue (~180–200 nm), Au (~100–150 nm), Ag (~60 nm) or gray (~30 nm). The recommended section thickness for embedded cells is between 50–100 nm (sections with a silver or light gold color).
! CAUTION Care should be taken to section at low speeds and to produce relatively thin sections. Accidentally moving the sample too close to the knife-edge during mounting or setting the section thickness too high can lead to severe damage of the expensive diamond knife.
! CAUTION It is best to create a very small area (preferably <1 mm^2) for optimal sections. A 35° knife (versus 45° or 55°) is recommended for producing less distortion owing to compression, curling or fracturing in biological samples.
? TROUBLESHOOTING

37| Produce a sufficient number of sections floating on the water surface.

38| Collect several sections onto a TEM grid (300-mesh Cu, with support film such as formvar/carbon), being careful to avoid the cutting edge of the knife.

39| Transfer sections by capillary action with a loop by allowing water to drain through the grid onto a piece of Whatman's filter paper placed below the grid. Alternatively, dip a grid under the sections, being careful to avoid folding of the sections.

40| Allow sections on grids to dry for a few minutes, then carefully place grids in a grid storage box using fine-tipped tweezers.
▲ CRITICAL STEP After using the diamond knife, take care to properly clean and store the knife. Avoid touching the cutting edge of the knife or washing it with any solvents; clean it with the tip of a polystyrene rod dipped in ethanol by lightly passing the rod over the edge of the knife. Alternatively, you can wash the knife in mild soapy water to remove dried-on sections and blow dry with pressurized air.
! CAUTION It is possible that NPs may embed into the diamond knife leading to damage over time. Careful inspection of the knife-edge or sections can reveal this problem.

Optional additional staining ● TIMING 30 min
41| Place pieces of parafilm (2 in²) in a glass petri dish, onto which add drops of water or stain.

42| Place the grid face down on a drop of ddH₂O for 1–2 min.

43| Transfer the grid face down onto a drop of 1% uranyl acetate (filtered through a 0.2-µm syringe filter) for 30 min.
? TROUBLESHOOTING

44| Dip the grid into a drop of ddH₂O to rinse.

45| Blot dry on Whatman's filter paper.

46| Place in a grid box until next stain is prepared.

47| Prepare another petri dish and parafilm, but add NaOH pellets to trap moisture.

48| Place the grid face down on a drop of lead citrate (Ultrostain 2) for 10 min, then quickly dip the grid in a drop of 0.1 M NaOH solution.
? TROUBLESHOOTING

49| Rinse the grid in a drop of ddH₂O and blot dry with filter paper.

50| Place in a grid box for storage until imaging.
! CAUTION Uranyl acetate is radioactive as well as carcinogenic; lead citrate is carcinogenic. Stains should not be prepared in ethanol or other solvents that may soften resin or degrade sections on the grids.
! CAUTION Do not reuse syringe filters as debris and precipitates can contribute to artifacts.
? TROUBLESHOOTING

Image with TEM ● TIMING 1–2 h
51| Image samples with the electron beam well spread to avoid damage to the delicate thin sections.

52| Collect images with micron bars and other pertinent information (kV, date, operator and so on) using digital software by Advanced Microscopy Techniques (AMT) or other software associated with the TEM.
! CAUTION If the sections appear unstable in the electron beam, they can be lightly coated with carbon. If the specimen appears to drift, thermal effects may be occurring. Care should be taken to ensure good thermal contact through the use of 300–400 mesh grids with carbon and formvar coating for stability, which reduces charging and increases conductivity.
? TROUBLESHOOTING

● TIMING
Step 1, Plate and grow cells: 24–48 h generally, depending on cells used and culture conditions
Steps 2–3, Prepare NP-dosing solutions: 30 min
Steps 4–6, Dose cells with NPs: 1–24 h
Steps 7–14, Cell processing: rinsing, pellet, fix, post-fix (stain) and dehydrate: 24 h
Step 15, Dehydration series: 5–15 min
Step 16–18, Resin embedding and curing: 24 h
Steps 19–28, Trimming of sample: 30 min–1 h
Steps 29–40, Thin sectioning: 30 min–1 h
Steps 41–50, Optional staining: 30 min
Steps 51–52, Imaging with TEM: 1–2 h

? TROUBLESHOOTING
Troubleshooting advice is provided in **Table 1**.

TABLE 1 | Troubleshooting table.

Step	Problem	Solution
1,4,7,10	Insufficient cells	Make sure that the pellet can be visualized (have enough cells—1 mm pellet) before embedding and that staining is sufficient (prepare fresh osmium stain), re-prepare sample with additional cells
1,7,10	Distortion of cell organelles	Reduce centrifugation speed, avoid agitation after osmium post-fixation as sample is very fragile, check pH of solutions within acceptable range 7.0–7.4, make sample smaller for more thorough penetration of the fixative or re-prepare sample with less cells
2,3	Contamination	Add antibiotics to dosing media, reduce dosing time, sterilize NPs by washing with ethanol or autoclaving
2–5	Nanoparticle (NP) agglomeration	Increase sonication time; add surfactants?
11	Production of myelin figures	Failure of aldehyde fixation to stabilize lipids, decrease fixation temperature, reduce fixation time, is a function of the lipid composition of the tissue
11–15	Evacuation of cell components	Prolonged fixation or dehydration (keep osmium fixation to <1 h for 1 mm pellet), use phosphate buffer to minimize extraction
13,14,43,48	Generation of heavy metal precipitates	Rinse well with ddH_2O after staining, use fresh stain and filters
15–18,52	Holes in sections	Insufficient embedment, check dehydration and embedding procedure
18	Samples are sticky or soft	Insufficient curing, check temperature and increase time
	Air bubbles in resin	Avoid vigorous mixing of resin components, consider resin reactions with water, warm resin mixture and apply light vacuum (use vacuum oven)
18,25,36	Section compression	Trim lower edge of block face shorter than top edge in a trapezoid shape, cure block longer to make harder and use lower clearance angle
	Section stripes or 'scoring'	Clean knife edge with warm soap and water (avoid solvents, which may degrade glue holding diamond in place), move to area on knife-edge without damage and use lower angle knife (e.g., 35°)
	Section ripples or 'chatter'	Avoid vibrations and drafts, move to different area on knife that is not blunt, reduce cutting speed and try different clearance angle
25,31	Block face wets after every turn and section may drag back over knife edge	Water level too high, try a few turns at high speed, static charging (use anti-static device or dryer sheets in area), block face is too large (trim smaller) and clearance angle is too low
41–50,52	Insufficient image contrast	Adjust digital image brightness and contrast settings; carry out optional post-staining with heavy metal stains
52	Sections unstable	Spread electron beam, reduce accelerating voltage to 75–80 kV and carbon coat grid

ANTICIPATED RESULTS

Typical micrographs of LR White-embedded thin sections of N2A cells that have internalized carbon-based NPs and were subsequently viewed with BF-TEM are shown in **Figure 6**. As a control measure, cells not incubated with NPs were imaged, as well as NPs alone (**Fig. 6d,e,i,j,n,o,s,t**). In the image of the representative control cell (**Fig. 6a**), a variety of features are noticeable, including the plasma membrane (PM), the nucleus (N), the mitochondria (M), the myelin whorl (W) and the vacuole (V). Artifacts such as knife marks (**Fig. 6b**) or osmium-based precipitates from the staining procedures are sometimes present. However, if there is concern that osmium precipitates are present, energy-dispersive X-ray (EDX) analysis can be carried out to distinguish artifacts owing to differences in their elemental composition compared with the NPs. In our studies, observing the presence of NPs in N2A cells contributed to our initial understanding of toxicity based on uptake and the uptake mechanism[9,13] (**Fig. 1**). The localization of NPs (e.g., CB, MWNT and SWNT, and NDs) in intracellular vacuoles after 24 h is evident at low magnifications (**Fig. 6b,f,k,q**). The membrane-bound cytoplasmic structures resembled endosomes owing to their light staining qualities and size of ~500 nm compared with phagosomes in cells, such as macrophages, which are typically >500 nm (ref. 88). Further evidence of an endocytic mechanism of entry was demonstrated in N2A cells exposed to NDs displaying evidence of plasma membrane invagination (**Fig. 6p**, arrow), which may occur in many other cell types[16,17,24,75]. Other sections revealed multiple endosomes containing NDs after 24 h (**Fig. 6q**, arrows).

Figure 6 | Overview of the uptake of carbon nanomaterials into neuroblastoma (N2A) cells after 24 h at 100 µg ml^{-1}. (**a**) Control N2A cell with selected intracellular features labeled mitochondria (M), plasma membrane (PM), nucleus (N), vacuole (V) and myelin whorl (W). (**b**) N2A cell incubated with carbon black (CB), which localized into an intracellular vacuole (arrow) as well as CB nanoparticles (NPs) outside the cell (white arrow) and a knife mark artifact through the section (*). (**c**) Higher magnification image of the CB NPs inside the vacuole. (**d**) Control CB NPs. (**e**) Higher magnification of control CB NPs. (**f**) N2A cell incubated with multi-walled carbon nanotubes (MWNTs), which localized into an intracellular vacuole (arrow). (**g**) Higher magnification image of MWNTs inside the N2A cell. (**h**) Higher magnification image of MWNTs inside the vacuole. (**i**) Control MWNTs. (**j**) Higher magnification of control MWNTs. (**k**) N2A cell incubated with single-walled carbon nanotubes (SWNTs), which localized into an intracellular vacuole (arrow). (**l**) Higher magnification image of SWNTs inside vacuole. (**m**) Different area in cell showing SWNTs inside vacuole (arrow). (**n**) Control SWNTs. (**o**) Higher magnification of control SWNTs. (**p**) N2A cell incubated with nanodiamonds (NDs) showing plasma membrane (PM) invagination suggestive of endocytic uptake (white arrow). (**q**) Localization of NDs to intracellular vacuoles (arrows) as well as in the cytoplasm (arrow heads). (**r**) Higher magnification of single vacuole containing NDs. (**s**) Control NDs. (**t**) Higher magnification of control NDs.
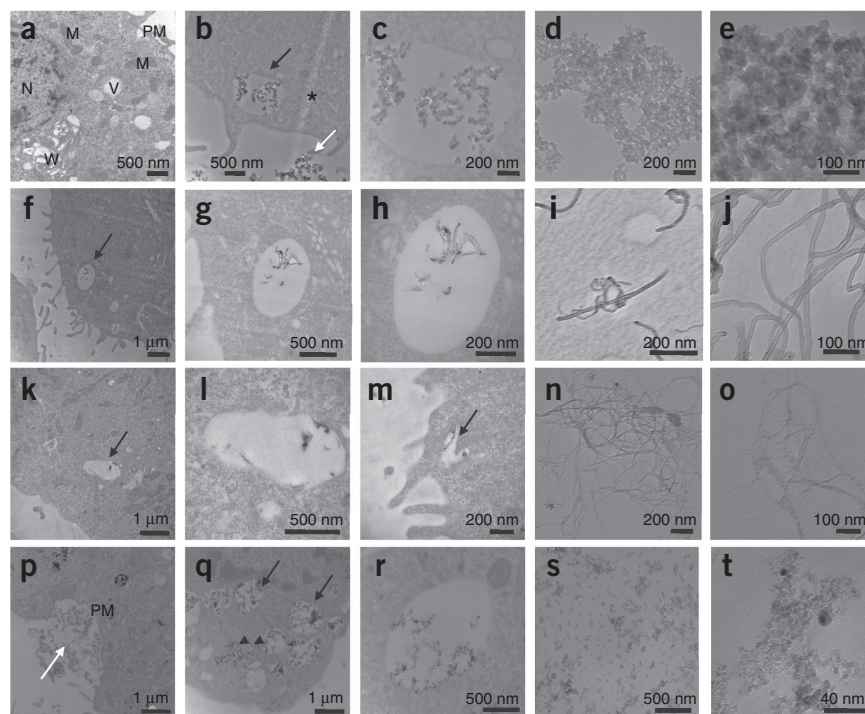
The presence of NDs in the cytoplasm without encapsulation in organelles was also demonstrated after 24 h, suggesting release from endosomes/lysosomes or alternative mechanisms of entry (**Fig. 6q**, arrowheads). Indeed, in other studies with macrophages, QDs were present both in the cytoplasm as small isolated groups and in larger coated vesicles[54]. The presence of clearly defined CB or MWNTs can be seen inside the endosomes (**Fig. 6c,h**) compared with SWNT bundles (**Fig. 6l,m**) or ND aggregates (**Fig. 6r**). The verification of these NPs was confirmed by comparing the morphology of the NP contained within endosomes (**Fig. 6c,h,l,m,r**) to the control NP images taken at similar magnifications (**Fig. 6d,i,n,s**) or in NP images at higher magnifications (**Fig. 6e,j,o,t**). The presence of residual metal catalyst particles in the MWNT or SWNT bundles inside the cells was readily visualized with dark, electron-dense contrast (**Fig. 6h,l,m**). However, it is well known that metallic and metal oxide NPs (e.g., Au, Ag, TiO$_2$ and SiO$_2$) generate much greater contrast in the TEM compared with the cellular background[13,14,16,17]. Therefore, this technique can be applied to a diverse range of cell types and NP compositions to determine NP ultrastructural localization with TEM.

AUTHOR CONTRIBUTIONS A.M.S. developed the protocol, carried out experiments, analyzed data and wrote the paper under the close supervision of S.M.H. and J.J.S. The carbon nanomaterials were provided by L.D. All the authors discussed the results and implications and commented on the manuscript.

1. Colvin, V.L. The potential environmental impact of engineered nanomaterials. *Nat. Biotechnol.* **21**, 1166 (2003).
2. Hoet, P.H., Nemmar, A. & Nemery, B. Health impact of nanomaterials? *Nat. Biotechnol.* **22**, 19 (2004).
3. Maynard, A.D. *et al.* Safe handling of nanotechnology. *Nature* **444**, 267 (2006).
4. Nel, A., Xia, T., Madler, L. & Li, N. Toxic potential of materials at the nanolevel. *Science* **311**, 622 (2006).
5. Hussain, S.M., Hess, K.L., Gearhart, J.M., Geiss, K.T. & Schlager, J.J. *In vitro* toxicity of nanoparticles in BRL 3A rat liver cells. *Toxicol. In Vitro* **19**, 975–983 (2005).
6. Braydich-Stolle, L., Hussain, S., Schlager, J.J. & Hofmann, M.-C. *In vitro* cytotoxicity of nanoparticles in mammalian germ-line stem cells. *Tox. Sci.* **88**, 412–419 (2005).
7. Hussain, S. *et al.* The interaction of manganese nanotubes with PC-12 cells induces dopamine depletion. *J. Tox. Sci.* **92**, 456–463 (2006).
8. Skebo, J.E., Grabinski, C.M., Schrand, A.M., Schlager, J.J. & Hussain, S.M. Assessment of metal nanoparticle agglomeration, uptake, and interaction using a high illuminating system. *Int. J. Tox.* **26**, 135–141 (2007).
9. Schrand, A.M. *et al.* Are diamond nanoparticles cytotoxic? *J. Phys. Chem. B.* **111**, 2–7 (2007a).
10. Schrand, A.M., Dai, L., Schlager, J.J., Hussain, S.M. & Osawa, E. Differential biocompatibility of carbon nanotubes and nanodiamonds. *Diam. Relat. Mater.* **16**, 2118–2123 (2007b).

11. Schrand, A.M. *et al.* Interaction and biocompatibility of multi-walled carbon nanotubes in PC-12 cells. *Int. J. Neuroprot. Neuroregener.* **3**, 115–121 (2007c).

12. Wagner, A.J. *et al.* Cellular interaction of different forms of aluminum nanoparticles in rat alveolar macrophages. *J. Phys. Chem. B.* **111**, 7353–7359 (2007).

13. Schrand, A.M., Braydich-Stolle, L.K., Schlager, J.J., Dai, L. & Hussain, S.M. Can silver nanoparticles be useful as potential biological labels? *Nanotechnology* **19**, 1–13 (2008a).

14. Carlson, C. *et al.* Uniques cellular interaction of silver nanoparticles: size-dependent generation of reactive oxygen species. *J. Phys. Chem. B.* **112**, 13608–13619 (2008).

15. Murdock, R.C., Braydich-Stolle, L., Schrand, A.M., Schlager, J.J. & Hussain, S.M. Characterization of nanomaterial dispersion in solution prior to in vitro exposure using dynamic light scattering technique. *Tox. Sci.* **101**, 239–253 (2008).

16. Braydich-Stolle, L.K. *et al.* Crystal structure mediates mode of cell death in TiO$_2$ nanotoxicity. *J. Nanopart. Res.* **11**, 1361–1374 (2008).

17. Yu, K.O. *et al.* Toxicity of amorphous silica nanoparticles in mouse keratinocytes. *J. Nanopart. Res.* **11**, 15–24 (2009).

18. Hussain, S.M. *et al.* Toxicity evaluation for safe use of nanomaterials: recent achievements and technical challenges. *Adv. Mat.* **21**, 1–11 (2009).

19. Schrand, A.M., Citan, S.A. & Shenderova, O.A. Nanodiamond particles: properties and perspectives for bioapplications. *Crit. Rev. Solid State Mater. Sci.* **34**, 18–74 (2009).

20. Colvin, V. The potential environmental impact of engineered nanomaterials. *Nat. Biotechnol.* **21**, 1166–1170 (2003).

21. Nel, A.E. *et al.* Understanding biophysicochemical interactions at the nano-bio interface. *Nat. Mater.* **8**, 543–557 (2009).

22. Ryman-Rasmussen, J.P., Riviere, J.E. & Monteiro-Rivere, N.A. Surface coatings determine cytotoxicity and irritation potential of quantum dot nanoparticles in epidermal keratinocytes. *Soc. Invest. Derm.* **127**, 143–153 (2006).

23. Zhang, L.W., Zeng, L., Barron, A.R. & Monteiro-Rivere, N.A. Biological interactions of quantum dot nanoparticles in skin and in human epidermal keratinocytes. *Tox. Appl. Pharm.* **228**, 200–211 (2008).

24. Zhang, L.W. & Monteiro-Rivere, N.A. Mechanisms of quantum dot nanoparticle cellular uptake. *Tox. Sci.* **110**, 138–155 (2009).

25. de Jonge, N., Peckys, D.B., Kremers, G.J. & Pistona, D.W. Electron microscopy of whole cells in liquid with nanometer resolution. *Proc. Natl. Acad. Sci. USA* **106**, 2159–2164 (2009).

26. Mayhew, T.M., Mühlfeld, C., Vanhecke, D. & Ochs, M. A review of recent methods for efficiently quantifying immunogold and other nanoparticles using TEM sections through cells, tissues and organs. *Ann. Anat.* **191**, 153–170 (2009).

27. Allen, T.D. *et al.* Visualization of the nucleus and nuclear envelope *in situ* by SEM in tissue culture cells. *Nat. Protoc.* **2**, 1180–1184 (2007).

28. Allen, T.D. *et al.* A protocol for isolating *Xenopus* oocyte nuclear envelope for visualization and characterization by scanning electron microscopy (SEM) or transmission electron microscopy (TEM). *Nat. Protoc.* **2**, 1166–1172 (2007).

29. Allen, T.D. *et al.* Generation of cell-free extracts of *Xenopus* eggs and demembranated sperm chromatin for the assembly and isolation of *in vitro*–formed nuclei for western blotting and scanning electron microscopy (SEM). *Nat. Protoc.* **2**, 1173–1179 (2007).

30. Wilhelm, C., Gazeau, F., Roger, J., Pons, J.N. & Bacri, J.C. Interaction of anionic superparamagnetic nanoparticles with cells: kinetic analyses of membrane adsorption and subsequent internalization. *Langmuir* **18**, 8148–8155 (2002).

31. Conner, S.D. & Schmid, S.L. Regulated portals of entry into the cell. *Nature* **422**, 37–44 (2003).

32. Shukla, R. *et al.* Biocompatibility of gold nanoparticles and their endocytotic fate inside the cellular compartment: a microscopic overview. *Langmuir* **21**, 10644–10654 (2005).

33. Kam, N.W.S., Liu, Z. & Dai, H. Carbon nanotubes as intracellular transporters for proteins and DNA: an investigation of the uptake mechanism and pathway. *Angew. Chem. Int. Ed.* **45**, 577–581 (2006).

34. Dobrovolskaia, M.A. & McNeil, S.E. Immunological properties of engineered nanomaterials. *Nat. Nanotech.* **2**, 469–478 (2007).

35. Verma, A. *et al.* Surface-structure-regulated cell-membrane penetration by monolayer-protected nanoparticles. *Nat. Mater.* **7**, 588–595 (2008).

36. Jin, H., Heller, D.A. & Strano, M.S. Single-particle tracking of endocytosis and exocytosis of single-walled carbon nanotubes in HIH3T3 cells. *Nano Lett.* **8**, 1577–1585 (2008).

37. Yu, J. *et al.* Effect of surface functionality of magnetic silica nanoparticles on the cellular uptake by Glioma cells in vitro. *J. Mater. Chem.* **19**, 1265–1270 (2009).

38. Geiser, M. *et al.* Ultrafine particles cross cellular membranes by nonphagocytic mechanisms in lungs and in cultured cells. *Environ. Health Perspect.* **113**, 1555–1560 (2005).

39. Porter, A.E. *et al.* Visualizing the uptake of C60 to the cytoplasm and nucleus of human monocyte-derived macrophage cells using energy-filtered transmission electron microscopy and electron tomography. *Enivron. Sci. Technol.* **41**, 3012–3017 (2007).

40. Porter, A.E. *et al.* Direct imaging of single-walled carbon nanotubes in cells. *Nat. Nanotechnol.* **2**, 713–717 (2007).

41. Cheng, C. *et al.* Toxicity and imaging of multi-walled carbon nanotubes in human macrophage cells. *Biomaterials* **30**, 4152–4160 (2009).

42. Steinbrecht, R.A. Freeze-substitution and freeze-drying. in *Cryotechniques in Biological Electron Microscopy* (eds. Steinbrecht, R.A. & Zierold, K.) 149–172 (K. Springer-Verlag, Berlin, 1987).

43. Parthasarathy, M.V. Chapter 5 freeze-substitution. *Methods Cell Biol.* **49**, 57–69 (1995).

44. Lucic, V. *et al.* Multiscale imaging of neurons grown in culture: from light microscopy to cryoelectron tomography. *J. Struct. Biol.* **160**, 146–156 (2007).

45. Satori, A. *et al.* Correlative microscopy: bridging the gap between fluorescence light microscopy and cryoelectron tomography. *J. Struct. Biol.* **160**, 135–145 (2007).

46. Hess, M.W., Muller, M., Debbage, P.L., Vetterlein, M. & Pavelka, M. Cryopreparation provides new insight into the effects of brefeldin A on the structure of the HepG2 Gel apparatus. *J. Struct. Biol.* **130**, 63–72 (2000).

47. Marko, M. Focused ion beam thinning of frozen hydrated biological specimens for cryoelectron microscopy. *Nat. Methods* **4**, 215–217 (2007).

48. Riley, M.R. *et al.* Comparison of the sensitivity of three lung derived cell lines to metals from combustion derived particulate matter. *Toxicol. In Vitro* **19**, 411–419 (2005).

49. Ricarda-Lorenz, M. *et al.* Uptake of functionalized, fluorescent-labeled polymeric particles in different cell lines and stem cells. *Biomaterials* **27**, 2820–2828 (2006).

50. Sayes, C.M., Reed, K.L. & Warheit, D.B. Assessing toxicity of fine and nanoparticles: comparing in vitro measurements to *in vivo* pulmonary toxicity profiles. *Toxicol. Sci.* **97**, 163–180 (2007).

51. Chang, J.-S., Chang, K.L.B., Hwang, D.-F. & Kong, K.-L. In vitro cytotoxicity of silica nanoparticles at high concentrations strongly depends on the metabolic activity type of the cell line. *Environ. Sci. Technol.* **41**, 2064–2068 (2007).

52. Xia, T. *et al.* Cationic polystyreen nanosphere toxicity depends on cell-specific endocytoic and mitohcondrial injury pathways. *ACS Nano* **2**, 85–96 (2008).

53. Lanone, S. *et al.* Comparative toxicity of 24 manufactured nanoparticles in human alveolar epithelial and macrophage cell lines. *Part. Fiber Toxicol.* **6**, 14–26 (2009).

54. Nabiev, I. *et al.* Non-functionalized nanocrystals can exploit a cell's active transport machinery delivering them to specific nuclear and cytoplasmic compartments. *Nano Lett.* **7**, 3452–3461 (2007).

55. Krüger, A. *et al.* Unusually tight aggregation in detonation nanodiamond: identification and disintegration. *Carbon* **43**, 1722–1730 (2005).

56. Greiner, N., Phillips, D., Johnson, J. & Volk, F. Dimaonds in detonation soot. *Nature* **333**, 440–442 (1998).

57. Liang, Y., Ozawa, M. & Krueger, A. A general procedure to functionalize agglomerating nanoparticles demonstrated on nanodiamond. *ACS Nano* **3**, 2288–2296 (2009).

58. Mei, B.C., Susumu, K., Medintz, I.L. & Mattoussi, H. Polyethylene glycol-based bidentate ligands to enhance quantum dot and gold nanoparticle stability in biological media. *Nat. Protoc.* **4**, 412–423 (2009).

59. Monteiro-Rivere, N.A., Inman, A.O., Wang, Y.Y. & Nemanich, R.J. Surfactant effects on carbon nanotube interactions with human epidermal keratinocytes. *Nanomedicine* **1**, 293–299 (2005).

60. Limbach, L.K. *et al.* Oxide nanoparticle uptake in human lung fibroblasts: effects of particle size, agglomeration, and diffusion at low concentrations. *Environ. Sci. Technol.* **39**, 9370–9376 (2005).

61. Shenderova, O. *et al.* Modification of detonation nanodiamonds by heat treatment in air. *Diamond Relat. Mater.* **15**, 1799 (2006).

62. Morita, Y. *et al.* A facile and scalable process for size-controllable separation of nanodiamond particles as small as 4 nm. *Small* **4**, 2154–2157 (2008).

63. Jamison, J.A. *et al.* Size dependent sedimentation properties of nanocrystals. *ACS Nano* **2**, 311–319 (2008).

64. Teeguarden, J.G., Hinderliter, P.M., Orr, G., Thrall, B.D. & Pounds, J.G. Particokinetics *in vitro*: dosimetry considerations for *in vitro* nanoparticle toxicity assessments. *Toxicol. Sci.* **95**, 300–312 (2007).

65. Jaiswal, J.K., Mattoussi, H., Mauro, J.M. & Simon, S.M. Long-term multiple color imaing of live cells using quantum dot bioconjugates. *Nat. Biotechnol.* **21**, 47–51 (2003).

66. Monteiro-Riviere, N.A., Nemanich, R.J., Inman, A.O., Wang, Y.Y. & Riviere, J.E. Multi-walled carbon nanotube interactions with human epidermal keratinocytes. *Toxicol. Lett.* **155**, 377–384 (2005).

67. Soto, K., Garza, K.M. & Murr, L.E. Cytotoxic effects of aggregated nanomaterials. *Acta Biomater.* **3**, 351–358 (2007).

68. Warheit, D.B., Webb, T.R., Sayes, C.M., Colvin, V.L. & Reed, K.L. Pulmonary instillation studies with nanoscale TiO_2 rods and dots in rats: toxicity is not dependent upon particle size and surface area. *Toxicol. Sci.* **91**, 227–236 (2006).

69. Stoeger, T. *et al.* Instillation of six different ultrafine carbon particles indicates a surface area threshold dose for acute lung inflammation in mice. *Environ. Health Perspect.* **114**, 328–333 (2006).

70. Elder, A. *et al.* Effects of subchronically inhaled carbon black in three species. I. Retention kinetics, lung inflammation, and histopathology. *Toxicol. Sci.* **88**, 614–629 (2005).

71. Brown, D.M., Wilson, M.R., MacNee, W., Stone, V. & Donaldson, K. Size dependent proinflammatory effects of ultrafine polystyrene particles: a role for surface area and oxidative stress in the enhanced activity of ultrafines. *Toxicol. Appl. Pharmacol.* **175**, 191–199 (2001).

72. Chithrani, B.D. & Chan, W.C.W. Elucidating the mechanisms of cellular uptake and removal of protein-coated gold nanoparticles of different sizes and shapes. *Nano Lett.* **7**, 1542–1550 (2007).

73. Nativo, P., Prior, I.A. & Brust, M. Uptake and intracellular fate of surface-modified gold nanoparticles. *ACS Nano* **2**, 1639–1644 (2008).

74. Gopee, N.V. *et al.* Migration of intradermally injected quantum dots to sentinel organs in mice. *Toxicol. Sci.* **98**, 249–257 (2007).

75. Gojova, A. *et al.* Induction of inflammation in vascular endothelial cells by metal oxide nanoparticles: effect of particle composition. *Environ. Health Perspect.* **115**, 403–409 (2007).

76. Gratton, S.E. *et al.* The effect of particle design on cellular internalization pathways. *Proc. Natl. Acad. Sci. USA* **105**, 11613–11618 (2008).

77. Vincent, A. *et al.* Protonated nanoparticle surface governing ligand tethering and cellular targeting. *ACS Nano* **3**, 1203–1211 (2009).

78. Karnovsky, M.J. A formaldehyde-glutaraldehyde fixative of high osmolality for use in electron microscopy. *JCB* **27**, 137A–138A (1965).

79. McDowell, E.M. & Trump, B.F. Histologic fixatives suitable for diagnostic light and electron microscopy. *Arch. Pathol. Lab. Med.* **100**, 405–414 (1976).

80. Monteiro-Riviere, N. & Inman, A. Challenges for assessing carbon nanomaterial toxicity to the skin. *Carbon* **44**, 1070–1078 (2006).

81. Rouse, J.G., Yang, J., Barron, A.R. & Monteiro-Riviere, N.A. Fullerene-based amino acid nanoparticle interactions with human epidermal keratinocytes. *Toxicol. In Vitro* **20**, 1313–1320 (2006).

82. Zhang, L.W., Zeng, L., Barron, A.R. & Monteiro-Riviere, N.A. Biological interactions of functionalized single-wall carbon nanotubes in human epidermal keratinocytes. *Int. J. Toxicol.* **26**, 103–113 (2007).

83. Zhang, Y. & Zhang, J. Surface modification of monodisperse magnetite nanoparticles for improved intracellular uptake to breast cancer cells. *J. Colloid Interface Sci.* **283**, 352–357 (2005).

84. Millonig, G. Advantages of a phosphate buffer for osmium tetroxide solutions in fixation. *J. Appl. Phys.* **32**, 1637 (1961).

85. Reynolds, E.S. Use of lead citrate at high pH as an electron-opaque stain in electron microscopy. *J. Cell Biol.* **17**, 208–212 (1963).

86. Graham, L. & Orenstein, J.M. Processing tissue and cells for transmission electron microscopy in diagnostic pathology and research. *Nat. Protoc.* **2**, 2439–2450 (2007).

87. Robards, A.W. & Wilson, A.J. *Procedure in Electron Microscopy: Module 5:5 Basic Biological Preparation Techniques for TEM* 5:5.1–5:5.28 (John Wiley & Son, Hoboken, NJ, 1999).

88. Aderem, A. & Underhill, D.M. Mechanisms of phagocytosis in macrophages. *Annu. Rev. Immunol.* **17**, 593–623 (1999).